Liquid crystal modulated optical CDMA in a fiber-based testbed

Yijing Fu*[1], Frank Barnes[1], Teresa Ewing[2], Steven Serati[2], and Xiao-Wei Xia[2]

[1]Department of Electrical Engineering and Optical Computing Systems Center

Campus Box 525, University of Colorado, Boulder, CO 80309

[2]Boulder Nonlinear Systems, Inc., 450 Courtney Way, Lafayette, CO 80026

* Yijing.Fu@colorado.edu

ABSTRACT

In recent years, optical CDMA systems have been proposed for multiple accesses to utilize the vast bandwidth available in optical fiber. Optical CDMA systems are believed to provide asynchronous access for each user in the system, which is especially suitable for usage in LAN. In this paper, we demonstrate a novel optical CDMA scheme in a fiber-based testbed. Using the liquid crystal spatial light modulator (SLM), we are able to construct a reconfigurable optical CDMA system suitable for fiber-optic networks. We address the code for each user in the spectrum domain by using a standard 4-f pulse shaping apparatus. Because of the low coherency of the light source we used in the system, we are able to modulate it in time domain without changing its frequency distribution significantly. We can reconfigure the network connection while keep the information bits un-influenced. Another merit of using analog liquid crystal device is that the transmissions of the different frequency components are analog controllable, we can get a uniform intensity distribution in frequency domain when the spectrum of the light source is not flat. Using the liquid crystal as a programmable optical modulator, the high polarization sensitivity of the components used in the system enables low crosstalk between different codes assigned to different users.

Keywords: Optical CDMA, LAN, fiber optical communication, liquid crystal, spatial light modulator

1. INTRODUCTION

Optical CDMA [1-4] techniques have been proposed for multiple access networks to utilize the vast bandwidth available in optical fibers. In an O-CDMA scheme, signals from all transmitters are distributed to every receiver using a star coupler. Each user receives all transmitted information, but is able to extract the signal of one particular transmitter from a background of multi-user interference using prior knowledge of the coding employed. Encoding and decoding processes are performed in the optical domain, eliminating any slowdown associated with optical-electronic conversion required in an electronic-based coding technology, a key motivation behind much of the work in O-CDMA. O-CDMA systems are believed to provide asynchronous access for each user, which is especially suitable for usage in LAN (local area networks). [5] In contrast to optical TDMA, which needs stringent synchronization, optical CDMA is able to provide asynchronous access for users. Also optical CDMA has an advantage over WDMA, since it eliminates the need for a stable wavelength source and the need for ultrafast tunable sources and filters in future optical packet-switched networks.

One of the great challenges in designing O-CDMA systems is selecting a set of optical address codes that have low periodic cross-correlation. The bipolar ({+1,-1}) nature of the codes is essential to achieving low cross-correlations and low multiple access interference. In a previous paper,[6] we presented an incoherent and reconfigurable bipolar coding scheme, using liquid crystal (LC) Spatial Light Modulators (SLMs) to encode the power spectrum of a broadband source into bipolar Walsh codes for data modulation. The key to our system performance depends on constructing a decoder that implements a true bipolar correlation using only unipolar signals and intensity detection. This has been accomplished using two unipolar correlations, followed by a subtraction.[7-8] The zero-shift cross correlation of two bipolar codes X and Y can be shown to be:

$$\Theta_{XY} = \sum_{i=0}^{N-1} X(i)Y(i) = \sum_{i=0}^{N-1} \left[U(i) - \overline{U}(i)\right]\left[V(i) - \overline{V}(i)\right] = J \cdot K - J \cdot \overline{K} \,. \qquad (1)$$

where the bipolar code is represented with two unipolar codes as $X(i) = U(i) - \overline{U}(i)$ and $Y(i) = V(i) - \overline{V}(i)$; $J = U \oplus \overline{U}$ and $K = V \oplus \overline{V}$ are the unipolar supercodes, both of length 2N formed by concatenating a sequence code and its complement. The operations $J \cdot K$ and $J \cdot \overline{K}$ are unipolar correlations and therefore can be performed optically.

In this paper, we present an incoherent and reconfigurable bipolar coding scheme based on a fiber testbed, using liquid crystal (LC) Spatial Light Modulators (SLMs). The usage of LC-SLM in the system provides reconfigurable codes assignment for each user. With high-speed nematic LC such as dual-frequency nematic LC material, the reconfiguration speed can be fast (sub-ms), which is an advantage for many applications. In addition, the non-uniform power spectrum of the broadband light source means the coding patterns are not uniform. By improving the uniformity of the power spectrum of the source, we are able to increase the code length, allowing more users to be supported. This is done by adjusting the intensity of each spectral chip independently via independent adjustment of the driving voltage for each pixel of the SLM.

2. SPECTRUM ENCODING

2.1 Implementation of Spectrum Encoding

Figure 1 shows an encoder setup to encode a signal into spectral bipolar codes. We address the code for each user in the spectrum domain by using a standard 4-f pulse shaping apparatus, composed of two gratings at the outer focal plane of a telescope. Single-mode optical fibers with appropriate collimators are used on all the light ports. The 1.5-µm Super Luminescent Diode (SLD) fiber output beam amplified via an EDFA is collimated via a GRIN lens (GL1) and diffracted by the grating (G1). The diffracted beam is collimated by a cylindrical lens (L1) of focal length 70 mm (with focal point at the grating). The collimated beam passes through the liquid crystal SLM that is between two crossed polarizers (P1 and P2). The pixelated liquid crystal elements are designed such that each wavelength channel can be driven independently. The coded channels are focused by the output lens (L2) and recombined by the output grating (G2) into a single beam that is coupled to output fiber via a GRIN lens (GL2). By adjusting the polarization direction of P1 and P2, and the holding voltage of the SLM, which determines the LC phase delay, the encoding contrast can be optimized. The modulated spectrum power can also be flattened by addusting the driving voltages applied on each individual pixel of the SLM.

Figure 2(a) shows the original power spectrum (dashed) of a SLD amplified by an EDFA, and the modulated power spectrum (solid) when the LC-SLM strips are set to the coding pattern of alternative on and off driven with equal binary voltages. An un-flattened spectral code of {0101010110101010} is achieved due to the spectral profile of the SLD source. When the LC-SLM strips are modulated in an analog way, a uniformed (flattened) spectrum modulation (solid) is achieved as shown in figure 2(b), compared with the un-flattened spectrum (dotted). The uniformity of the coding spectrum is greatly improved, which will lead to better performance of the O-CDMA system.

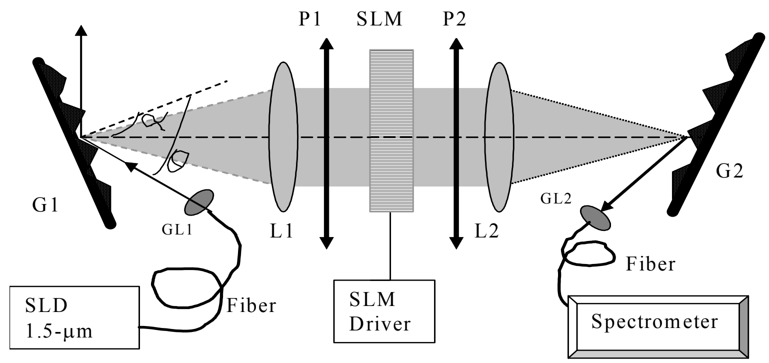

Fig. 1: Spectral encoding of the SLD spectrum via a SLM

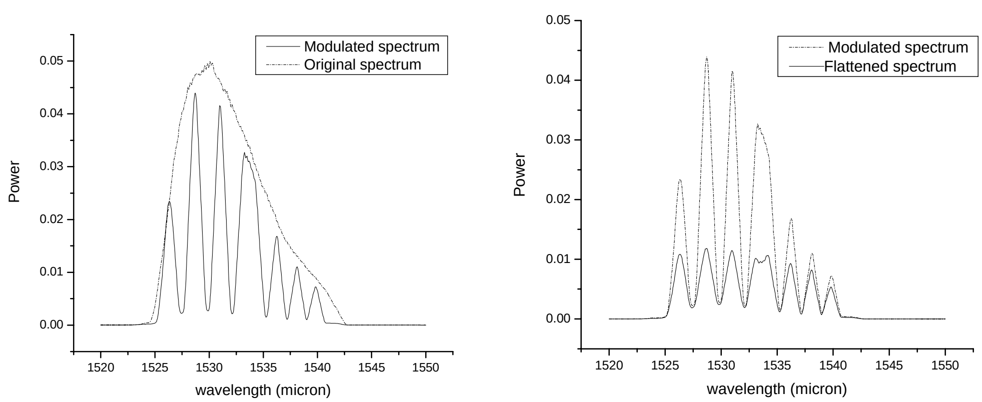

Fig. 2: Original and modulated (un-flattened and flattened) power spectra of the EDFA amplified SLD via a SLM

2.2 Encoding System Analyses

The light source we used in the system is a SLD amplified by an EDFA, the coherent length of this kind of the light source is only a few millimeters, and thus we need to develop a more general approach than the monochromatic one to analyze the system. We will utilize the mutual coherent function propagation in free space to analyze the transmission characteristic of the optical system. [9]

To describe the source plane and the image plane of the optical system, let $Q_1(\xi_1, \eta_1)$, $Q_2(\xi_2, \eta_2)$ represent two points on the source plane, and $P_1(x_1, y_1)$, $P_2(x_2, y_2)$ represent two points on the image plane, respectively. We also introduce two complex vectors $X = \{x_1, y_1, ix_2, iy_2\}$ and $\rho = \{\xi_1, \eta_1, i\xi_2, i\eta_2\}$ by defining the following:

$$\begin{aligned} X\rho &= x_1\xi_1 + y_1\eta_1 - x_2\xi_2 - y_2\eta_2 \\ X^2 &= x_1^2 + y_1^2 - x_2^2 - y_2^2 \\ \rho^2 &= \xi_1^2 + \eta_1^2 - \xi_2^2 - \eta_2^2 \end{aligned} \tag{2}$$

The mutual spectral density G is the Fourier-transform of the mutual coherent function. The propagation of mutual spectral density between two planes in free space can be described as: [9-10]

$$G(X,\nu) = \frac{\nu^2}{c^2 z^2} \int G(\rho,\nu) \exp[\frac{i\pi\nu}{cz}(X-\rho)^2] d\rho \ , \tag{3}$$

where ν is the frequency, c is the speed of light, and z is the propagation distance between two planes.

For the propagation of mutual spectral density in the scheme depicted in figure 1, let $t_m(x,\nu)$ be the mask transfer function of the SLM and $T_m(X,\nu) = t_m(x_1,\nu) t_m{}^*(x_2,\nu)$, then the mutual spectral intensity at the output can be shown to be:

$$G(\rho',\nu) \ = \ \frac{\nu^4}{c^4 F^4} \int\int G_{in}(\beta\rho,\nu)\beta \exp(i\gamma\Omega(\xi_1 - \xi_2)) \exp(-i\frac{2\pi\nu}{cF} X\rho) T_m(X,\nu) \exp(-i\frac{2\pi\nu}{cF} X\rho') dX d\rho \tag{4}$$

where F is the lens focal length, and the mutual coherent function of the incident beam can be written as:

$$G_{in}(\rho,\nu) \ = \frac{2}{\Delta\nu_0\sqrt{\pi}} \exp(-\frac{(\nu-\nu_0)^2}{(\Delta\nu\ )^2}) \frac{2P^0}{\pi r_V^2} \exp(-\frac{\xi_1^2 + \eta_1^2}{r_V^2}) \exp(\frac{\xi_2^2 + \eta_2^2}{r_V^2}) \ , \tag{5}$$

using a simplified model of the incident beam satisfying Gaussian distribution written in the form of:

$$u(\xi,\eta) = \sqrt{\frac{2P^0}{\pi r_V^2}} \exp(-\frac{\xi^2 + \eta^2}{r_V^2}) \ , \tag{6}$$

while r_V is the radius of the incident light beam, P^0 is the incident power , ν_0 is the central wavelength and $\Delta\nu$ the bandwidth of the spectrum.
In the equation above, we also used the transfer function of an optical grating for a coherent wave field : [10]

$$E_{out}(x,\omega) = \sqrt{\beta}E_{in}(\beta x,\Omega)\exp(i\gamma\Omega x) \tag{7}$$

where:

$$\beta = \cos(\theta_i)/\cos(\theta_d) \qquad \gamma = 2\pi/\overline{\omega}d\cos(\theta_d) \qquad \Omega = \omega - \overline{\omega}$$

with θ_i and θ_d being the incident angle and the diffracted angle, respectively, and d the grating period, ω the angular frequency, $\overline{\omega}$ the central angular frequency.

We calculated the transmission efficiency for different wavelengths under different SLM pitch sizes. Figure 3 shows the results at SLM pitch sizes of 300 μm and 150 μm, respectively. The LC-SLM strips are set to the alternative on–and-off coding pattern, and the following parameters close to the experiment are used:

$$\nu_0 = 1.53\mu m$$
$$\Delta\nu_0 = 10nm$$
$$r_V = 2.5mm$$
$$F = 70mm$$
$$\theta_i = 62^O$$

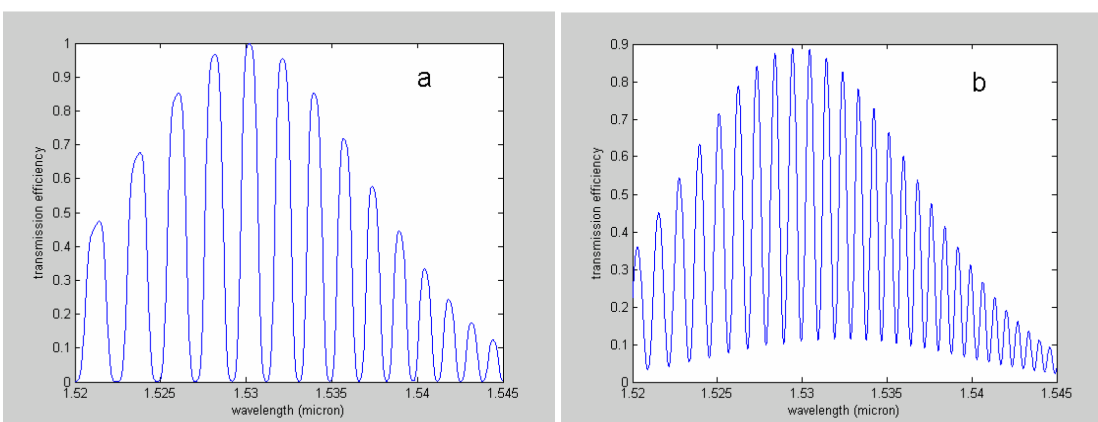

Fig. 3: Transmission characteristics of the encoding system: a): transmission at LC strip width = 300 μm; b): transmission at LC strip width = 150 μm

It can be seen that the modulation depth of the transmitted spectrum increases with the strip width of the LC-SLM. A good modulation extinction ratio can be achieved with a strip width of 300 μm. In our experiments, we typically choose a large strip width of 400 μm, to ensure good modulation of the power spectrum.

3. SPECTRUM DECODING

We built a fiber-based spectrum encoder/decoder pair as shown in Figure 4. The power spectrum of the incoming light beam is divided into 16 slices, or chips, and encoded into J pattern by programming the one-dimensional SLM1 as shown in Figure 2 for a code pattern of {0101010110101010}. The encoded power spectrum is coupled into a single-mode fiber by a collimation lens and then sent to the decoder via a fiber. The encoded light passes SLM2 with a pattern corresponding to K, the code selected for detection. With the polarization of J code being 45° to the axis (vertical) of SLM2, the transmitted light of SLM2 consists of two orthogonal components being +45° and –45° from the SLM2 axis and producing signals proportional to $J \cdot K$ and $J \cdot \overline{K}$, respectively. The two light components are rotated by a polarization rotator (PR) 45° to perpendicular and parallel polarization state. The beam is then focused by lens and diffracted by a grating into collimated beams. A polarization beam splitter (PBS) cube can then separate the two signals proportional to $J \bullet K$ and $J \bullet \overline{K}$ into two beams. These two beams are coupled back into two fibers and measured by photo detectors. When a balanced detection method is used, the photodetector currents are subtracted from each other, and the resulting signal is proportional to the bipolar correlation Θ_{XY} of Eq. (1).

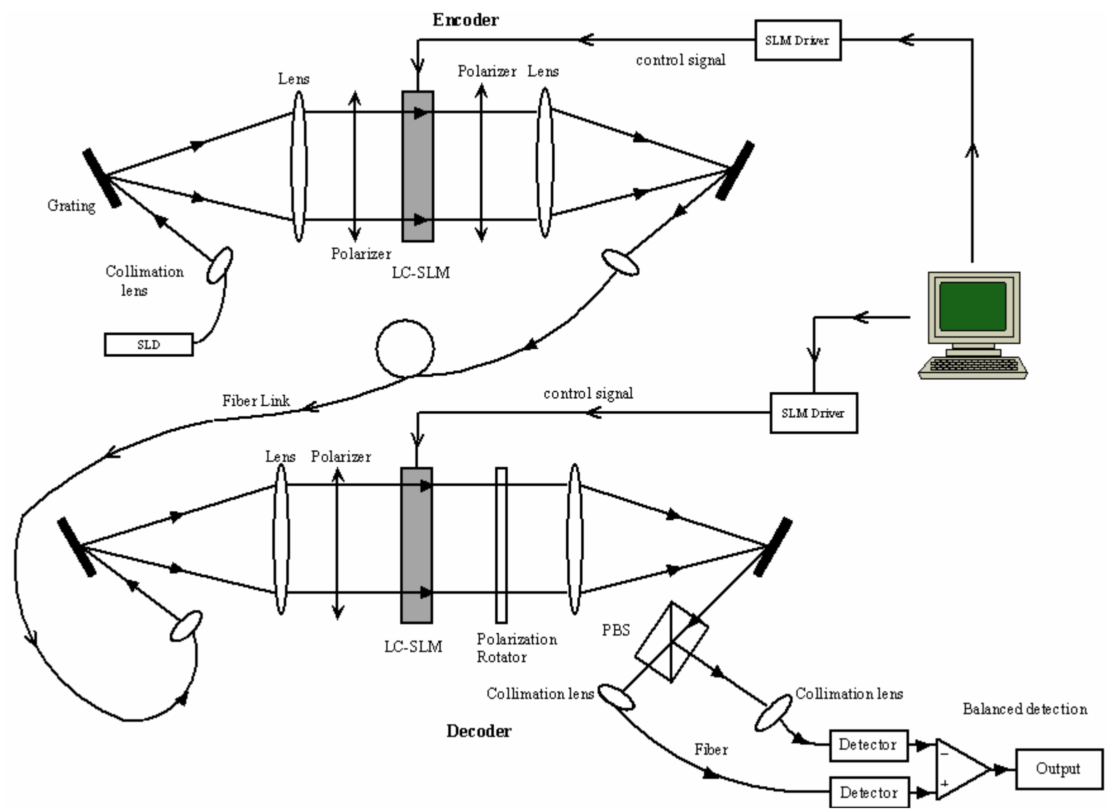

Fig. 4: Fiber-based testbed for spectrum encoding and decoding.

In a local area network, the received signal will be a superposition of spectra corresponding to the entire set of active user's codes. Since the receiver is linear in optical power, the output will be a superposition of their correlations with the desired code. A sequence of signals from the desired user will produce large value Θ_{XY} or $-\Theta_{XY}$. The interference between the desired user and other users is suppressed using bipolar codes to near zero, or very low magnitude as in Walsh or Gold codes. The high polarization selectivity of these bulk components coupled with the polarization rotation ability of liquid crystal elements makes switching possible with high extinction ratio and low crosstalk.

During the experiment, the two SLMs needed to be first aligned spatially with each other, to get the same modulation of the power spectrum. After the SLMs were aligned, the power difference of the two light components (i.e. correlation) was measured. Four orthogonal codes (and their conjugates) are chosen: $J1$={11001100 00110011}, $J2$={11110000 00001111}, $J3$={10011001 01100110}, $J4$={01010101 10101010}and their complex conjugates $\overline{J}_1$, $\overline{J}_2$, $\overline{J}_3$, $\overline{J_4}$. The encoder SLM1 was fixed to code J_4, while the coding pattern of the decoder SLM2 varied to transmit any of the code sequences, J_1, J_2, J_3, J_4 $\overline{J}_1$, $\overline{J}_2$ $\overline{J}_3$ and $\overline{J_4}$. Figure 5 shows the correlations between the codes that were measured for the encoder SLM1 set to $J4$ with the above single-user configuration. It can be seen that only when the matched codes $J4$ or $\overline{J}4$ is set for SLM2, the decoder responds with a large positive or negative correlation signal. Good contrast between the autocorrelation and cross correlation values shows that a binary information symbol can be recovered by an appropriate threshold operation, demonstrating the feasibility of encoding and decoding for this fiber-based optical array CDMA system.

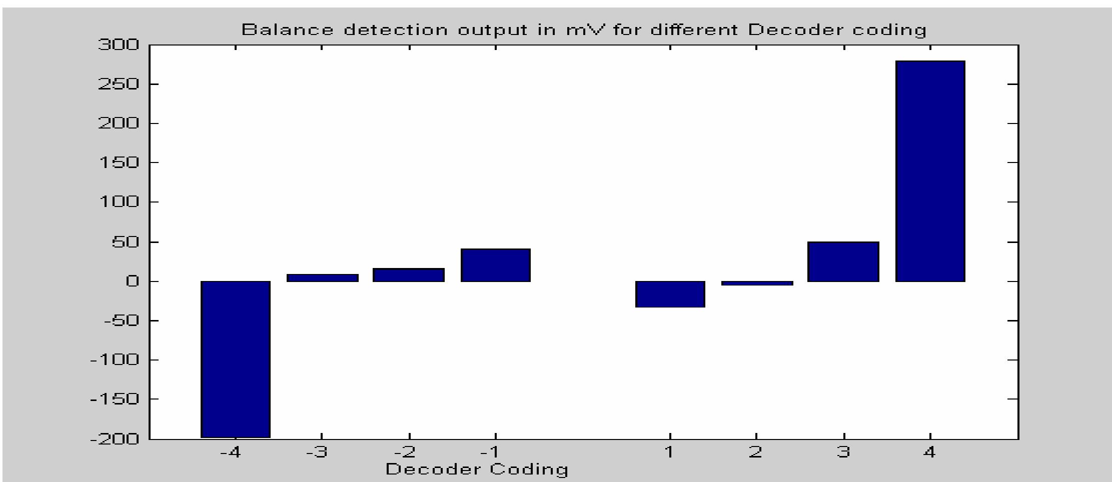

Fig. 5: Measured correlation values of the codes. The encoder SLM1 pattern was fixed as J4, while the decoder SLM2 sent all the patterns sequentially (J1, J2, J3, J4 [1,2,3,4] and their complex conjugates [-1,- 2, -3, -4]).

4. CONCLUSION

We have demonstrated a reconfigurable encoder-decoder system based on a fiber test-bed using liquid crystal spatial light modulators. A broadband Super Luminescent Diode source amplified by an EDFA has been spectrally encoded and decoded. The bipolar correlations of the codes are verified. Good contrast between the autocorrelation and cross correlation values shows that a binary information symbol can be recovered by an appropriate threshold operation.

ACKNOWLEDGMENTS

This research was funded through Air Force Office of Scientific Research (AFOSR) Contract F49620-02-C-0021.

REFERENCES

1. D. D. Sampson, G. J. Pendock, and R. A. Griffin, "Photonic code-division multiple-access communications, " *Fiber and Integ. Opt.* , **16**, p.129, 1997.

2. H.P. Sardesai, C.-C. Chang, and A.M. Weiner, "A femtosecond code-division multiple-access communication system testbed," *Journal of Lightwave Technology*, **16**, pp.1953-1964, 1998

3. A. Grunnet-Jepsen, A. E. Johnson E. S. Maniloff, T. W. Mossberg, M. J. Munroe, and J. N. Sweetser, "Demonstration of all-fiber sparse lightwave CDMA based on temporal phase encoding," *IEEE Photon. Tech. Letts.*, **11**, pp.1283-1285, 1999.

4. L. R. Chen and P. W. E. Smith, "Demonstration of incoherent wavelength-encoding/time–spreading optical CDMA using chirped moiré gratings," *IEEE Photon. Tech. Letts.*, **12**, p.1281, 2000.

5. Paul R.Prucnal, Mario A. Santoro, Ting Rui Fan, "Spread spectrum Fiber-Optic Local Area Network Using Optical Processing," *J. of Lightwave Tech*., **LT-4**, p.547, May 1986

6. Xiao-Wei Xia, Teresa K. Ewing, Steven A. Serati, Yijing Fu, Rong Zhou, John A. Neff, and Frank S. Barnes, "Demonstration of reconfigurable O-CDMA using liquid crystal modulators," in *Active and Passive Optical Components for WDM Communications III*, Achyut K. Dutta, Abdul Ahad S. Awwal, Niloy K. Dutta, Kazuo Fujiura, Editors, *Proc. SPIE*, Vol. **5246** (2003), Pp.95-102.

7. L. Nguyen, T. Dennis, B. Aazhang, and J. F. Young, "Experimental demonstration of bipolar codes for optical spectral amplitude CDMA communication," *J. of Lightwave Tech*., **15**, p.1647, 1997

8. T. Dennis and J. F. Young, "Measurements of BER performance for bipolar encoding of an SFS," *J. of Lightwave Tech*., **17**, p.1542, 1999

9. V. Morozov, J. Neff, and H. Zhou, "Signal and noise analysis in free-space interconnects," *J. Opt. Soc. Am. A*, **14**, p. 859, 1997

10. Marc M. Wefers and Keith A. Nelson, "Space-Time Profiles of Shaped Ultrafast Optical Waveforms," *IEEE J. of Quantum Electronics*, **32**, p. 161, Jan 1996